NJC

ROYAL SOCIETY OF CHEMISTRY

PAPER

View Article Online
View Journal | View Issue

Cite this: *New J. Chem.*, 2023, **47**, 17679

Effect of water-soluble zinc porphyrin on the catalytic activity of fumarase for L-malate dehydration to fumarate†

Mika Takeuchi[a] and Yutaka Amao *[ab]

Fumarase from porcine heart (FUM; EC 4.2.1.2) is an enzyme that dehydrates L-malate in an aqueous medium to catalyze fumarate production. In the visible-light driven NADH regeneration with the system of an electron donor, water-soluble zinc porphyrin as a photosensitizer and pentamethylcyclopentadienyl rhodium 2,2′-bipyridine complex ($[Cp^*Rh(bpy)(H_2O)]^{2+}$) and malate dehydrogenase from *Sulfobus tokodaii* (oxaloacetate-decarboxylating; MDH; EC 1.1.1.38), fumarate can be produced from CO_2 and pyruvate by dehydrating L-malate produced as an intermediate with FUM. To improve fumarate production efficiency in this system, it is necessary to study the interaction between FUM and water-soluble zinc porphyrin. In this work, the effect of water-soluble zinc or metal-free porphyrin derivatives, tetra(4-sulfonatophenyl)porphyrin, tetra-(4-carboxyphenyl)porphyrin, tetrakis(4-methylpyridyl)porphyrin or tetrakis(4-*N*,*N*,*N*-trimethylaminophenyl)-porphyrin on the catalytic activity of FUM for L-malate dehydration to fumarate was studied. It was found that the addition of anionic water-soluble zinc porphyrins, zinc tetra(4-sulfonatophenyl)porphyrin ($ZnTPPS^{4-}$) and zinc tetra(4-carboxyphenyl)porphyrin ($ZnTCPP^{4-}$) inhibited the catalytic activity of FUM. In particular, fumarate production with FUM was strongly suppressed in the addition of $ZnTPPS^{4-}$ (reduced to about 16% compared to control experiments). On the other hand, the addition of cationic water-soluble zinc or metal-free porphyrins had little effect on the catalytic activity of FUM for L-malate dehydration to fumarate. Furthermore, UV-vis absorption and circular dichroism spectroscopic results suggested that $ZnTPPS^{4-}$ binds to the substrate-binding site of FUM and inhibits fumarate production.

Received 23rd June 2023,
Accepted 6th September 2023

DOI: 10.1039/d3nj02900j

rsc.li/njc

Introduction

Fumarate, an unsaturated dicarboxylic acid, is a chemical building block with many applications, including in the biodegradable engineering polymer industry.[1–5] In the field of polymer engineering chemistry, fumarate is useful as a precursor for biodegradable plastic poly(butylene succinate) (PBS).[6–10] Fumarase (FUM) is an enzyme that catalyzes the reversible hydration/dehydration of fumarate to L-malate, as shown in Fig. 1.[11–17] Generally, in an aqueous medium, an intermolecular or intramolecular dehydration proceeds only in the presence of a strong acid or base catalyst. On the other hand, FUM catalyzes fumarate production based on L-malate dehydration in an aqueous medium without the need for a strong acid or base catalyst.

Furthermore, L-malate is synthesized from pyruvate and CO_2 in the presence of NADH as a co-enzyme by the catalytic function of malate dehydrogenase (NAD^+-dependent oxaloacetate-decarboxylating; MDH).[18–23] Thus, by using the dual catalysts system of FUM and MDH, it is possible to synthesize fumarate as a raw material for biodegradable or engineering plastics from pyruvate and CO_2 in the presence of NADH, as shown in Fig. 2.

We previously reported the fumarate synthesis from pyruvate and bicarbonate formed by dissolving CO_2 in an aqueous medium in the presence of NADH with the dual catalysts system of FUM from porcine heart (EC 4.2.1.2) and MDH from *Sulfobus tokodaii*, oxaloacetate-decarboxylating; (EC 1.1.1.38), as shown in Fig. 2.[24] We also have found that the addition of phosphate improves the L-malate dehydration catalytic function

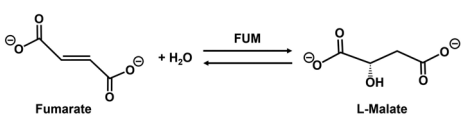

Fig. 1 The reversible hydration/dehydration of fumarate to L-malate with FUM.

[a] *Graduate School of Science, Osaka Metropolitan University, 3-3-138 Sugimoto, Sumiyoshi-ku, Osaka 558-8585, Japan*
[b] *Research Centre of Artificial Photosynthesis (ReCAP), Osaka Metropolitan University, 3-3-138 Sugimoto, Sumiyoshi-ku, Osaka 558-8585, Japan. E-mail: amao@omu.ac.jp*

† Electronic supplementary information (ESI) available. See DOI: https://doi.org/10.1039/d3nj02900j

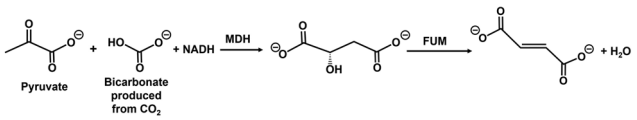

Fig. 2 Fumarate synthesis from pyruvate and CO_2 with the dual catalysts (FUM and MDH) in the presence of NADH.

of FUM in this system.[25] Since the expensive biological reagent NADH acts as a sacrificial reagent in the system of Fig. 2, it is desirable to incorporate a means of NADH regeneration to the catalytic system. Many hybrid systems of visible-light driven NADH regeneration consisting of an electron donor, a photosensitizer and pentamethylcyclopentadienyl rhodium bipyridine complex ($[Cp^*Rh(bpy)(H_2O)]^{2+}$), and various oxidoreductases including formate, lactate, 3-hydroxybutyrate dehydrogenases have been reported.[26–34] We also reported the visible-light driven fumarate synthesis from pyruvate and bicarbonate with the hybrid system of NADH regeneration by triethanol amine (TEOA) as an electron donor, water-soluble zinc tetra(4-sulfonatophenyl)porphyrin ($ZnTPPS^{4-}$) as a photosensitizer, and $[Cp^*Rh(bpy)(H_2O)]^{2+}$, and the dual catalyst of FUM and MDH as shown in Fig. 3.[35] After 5 h of reaction time, the concentration of fumarate to intermediate L-malate ratios in the systems shown in Fig. 2 and 3 are estimated to be 0.38 and 0.24, respectively. The system shown in Fig. 3 incorporates visible light-driven NADH regeneration, resulting in lower intermediate L-malate production compared to the system with NADH as a sacrificial reagent in Fig. 2. However, in both systems, only 24% of the L-malate is converted to fumarate in the system in Fig. 3, even though there is still excess L-malate relative to the fumarate produced. This indicates that fumarate production based on the FUM-catalyzed dehydration of L-malate is influenced by the compounds comprising Fig. 3. In the above-mentioned hybrid systems of visible-light driven NADH regeneration and oxidoreductases, the main subject has been the efficiency of NADH production, and the interaction between dye molecules and enzymes has not been the focus yet. In other words, it is necessary to ascertain the influence of dye molecules used in the system shown in Fig. 3 on the catalytic function of FUM. In order to improve fumarate production efficiency in the system shown in Fig. 3, moreover, it is necessary to investigate the interaction between FUM and water-soluble zinc porphyrin.

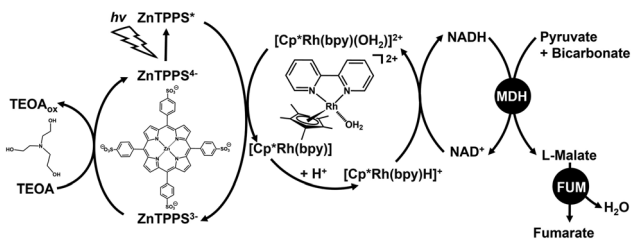

Fig. 3 Visible-light driven fumarate production from pyruvate and bicarbonate *via* L-malate as an intermediate with the combination of NAD^+ reduction system of TEOA as an electron donor, $ZnTPPS^{4-}$ as a photosensitizer and $[Cp^*Rh(bpy)(H_2O)]^{2+}$, and dual biocatalysts (MDH and FUM).

In this work, the effect of water-soluble porphyrin derivatives (chemical structures shown in Fig. 4) on the catalytic activity of FUM for L-malate dehydration to fumarate was investigated. Furthermore, the interaction between FUM and water-soluble porphyrin derivatives was investigated by UV-vis absorption and circular dichroism spectroscopic techniques.

Experimental

Materials

$ZnTPPS^{4-}$ was purchased from Frontier Scientific Inc. Tetra(4-sulfonatophenyl)porphyrin (H_2TPPS^{4-}), tetra(4-carboxyphenyl)-porphyrin (H_2TCPP^{4-}) and tetrakis(4-methylpyridyl)porphyrin (H_2TMPyP^{4+}) were purchased from Tokyo Chemical Industry Co., Ltd. Tetrakis(4-*N,N,N*-trimethylaminophenyl)porphyrin (H_2TMAP^{4+}) was purchased from Sigma-Aldrich Co. LLC. Fumarase (FUM) from porcine heart (EC 4.2.1.2; molecular weight: 200 kDa)[36,37] was obtained from Merck Co., Ltd. One activity unit of FUM convert 1.0 μmol of L-malate to fumarate in potassium phosphate buffer per min at pH 7.6 at 25 °C. The other chemicals were of analytical grade or the highest grade available obtained from FUJIFILM Wako Pure Chemical Corporation or NACALAI TESQUE, INC. $ZnTCPP^{4-}$, $ZnTMAP^{4+}$ and $ZnTMPyP^{4+}$ were synthesized by refluxing respective metal-free porphyrins with about 5 times molar equivalent of zinc acetate in the methanol solution according to the previous report.[38–42] The insertion of zinc into the porphyrin ring was confirmed by the change in the Q band of each porphyrin in the UV-visible absorption spectrum (SHIMADZU, MaltiSpec-1500).

Fumarate production with FUM in the presence of water-soluble porphyrin derivatives

The reaction mixture consisted of sodium L-malate (1.0 mM) and zinc or metal-free porphyrin (10 μM) in 5.0 mL of 500 mM 4-(2-hydroxyethyl)-1-piperazineethanesulfonic acid (HEPES)-NaOH buffer (pH 7.8). The reaction was started by adding FUM (0.5 units; 1.3 nM) to this solution with a thermostatic chamber set at a temperature of 30.5 °C. The total volume of

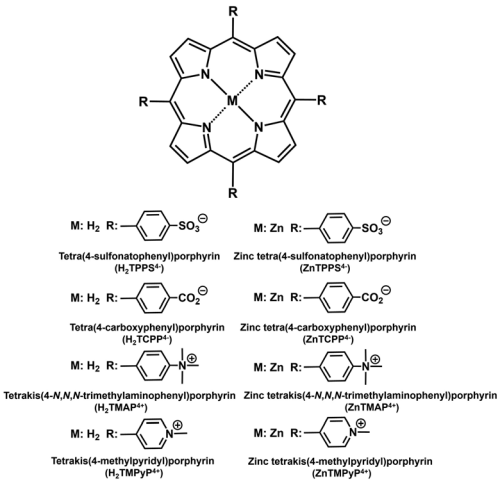

Fig. 4 Chemical structures of water-soluble porphyrin derivatives.

reaction vessel is 6.0 mL. The amount of fumarate produced was determined by ion chromatography (Metrohm, Eco IC; electrical conductivity detector) with an ion exclusion column (Metrosep Organic Acids 250/7.8 Metrohm; column size: 7.8 × 250 mm; composed of 9 μm polystyrene-divinylbenzene copolymer with sulfonic acid groups). Details of fumarate quantification by ion chromatograph are described in the supporting information. The fumarate concentration was determined from the calibration curve based on the chromatogram of a standard sample (Fig. S1, ESI†) using the eqn (S1).

UV-vis absorption spectrum measurement for the solution of FUM in the presence of water-soluble zinc porphyrin derivatives

UV-vis absorption spectra of the solution of $ZnTPPS^{4-}$ or $ZnTMAP^{4+}$ (10 μM) and FUM (0.5 units; 1.3 nM) in 2.0 mL of 500 mM HEPES buffer solution (pH 7.8) were measured using UV-visible absorption spectroscopy (SHIMADZU, MaltiSpec-1500). UV-vis absorption spectra of $ZnTPPS^{4-}$ and $ZnTMAP^{4+}$ in the absence of FUM also were measured as the reference samples.

Circular dichroism spectroscopy measurement for the solution of FUM in the presence of water-soluble zinc porphyrin derivatives

Circular dichroism (CD) spectra in near-UV region of FUM (0.75 μM; the mean residual weight; 110[37]) in the presence of $ZnTMAP^{4+}$ or $ZnTPPS^{4-}$ were measured using a J-720W spectropolarimeter (JASCO) with a 1.0-nm excitation bandwidth at 4 °C. CD spectra of FUM, $ZnTPPS^{4-}$ and $ZnTMAP^{4+}$ also were measured as the reference samples.

Results and discussion

Fumarate production with FUM in the presence of water-soluble zinc porphyrin derivatives

Fig. 5 shows the time dependence of concentration of fumarate produced with FUM in the presence of various zinc porphyrin derivatives (The ion chromatograph chart during the reaction is shown in Fig. S2(a)–(d), ESI†).

As shown in Fig. 5, no change in the fumarate production from L-malate with FUM by addition of cationic zinc porphyrins, $ZnTMPyP^{4+}$ or $ZnTMAP^{4+}$ was observed. By addition of anionic zinc porphyrins, $ZnTCPP^{4-}$ or $ZnTPPS^{4-}$, on the other hand, the fumarate production from L-malate with FUM was suppressed. Especially, the fumarate production with FUM was strongly suppressed in the presence of $ZnTPPS^{4-}$. These results suggested that the sulfo group bonded to the zinc porphyrin had a stronger effect on the catalytic activity of FUM than the carboxy group.

Fumarate production with FUM in the presence of water-soluble metal-free porphyrin derivatives

Next, let us focus on the effect of zinc coordinated to porphyrins on the catalytic activity of FUM for L-malate dehydration to produce fumarate. FUM-catalyzed fumarate production was investigated in the presence of metal-free porphyrin derivatives. Fig. 6 shows the time dependence of concentration of fumarate

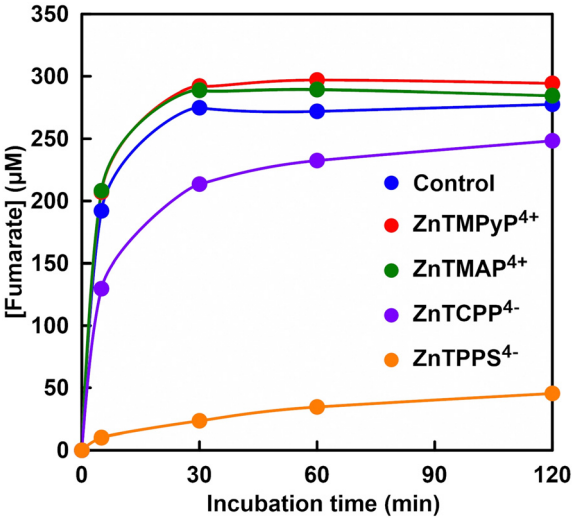

Fig. 5 Time dependence of fumarate production from L-malate (1.0 mM) with FUM (0.5 units; 1.3 nM) in the presence of zinc porphyrin (10 μM). ●: control; ●: $ZnTMPyP^{4+}$; ●: $ZnTMAP^{4+}$; ●: $ZnTCPP^{4-}$; ●: $ZnTPPS^{4-}$.

produced with FUM in the presence of various metal-free porphyrin derivatives (The ion chromatograph chart during the reaction is shown in Fig. S3(a)–(d) (ESI†). As shown in Fig. 6, no change in the fumarate production from L-malate with FUM by addition of cationic metal-free porphyrins, H_2TMPyP^{4+} or H_2TMAP^{4+} also was observed. By addition of anionic metal-free porphyrins, H_2TCPP^{4-} or H_2TPPS^{4-}, on the other hand, the fumarate production with FUM also was inhibited. Especially, the fumarate production with FUM was suppressed in the presence of H_2TPPS^{4-}, compared with that of H_2TCPP^{4-}. These results suggested that the sulfo group bonded to the metal-free porphyrin also was affected on the catalytic activity of FUM than the carboxy group.

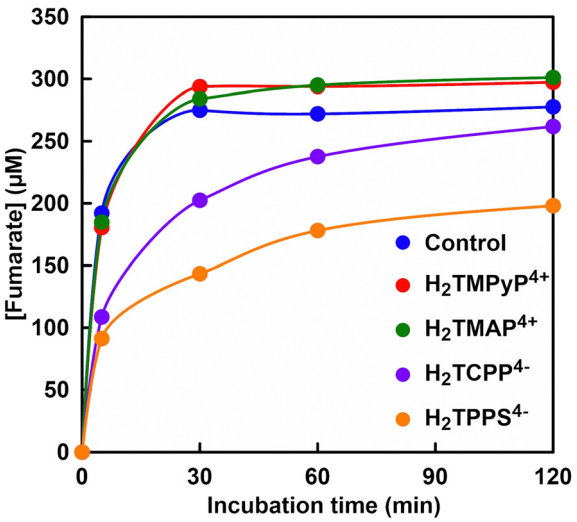

Fig. 6 Time dependence of fumarate production from L-malate (1.0 mM) with FUM (0.5 units; 1.3 nM) in the presence of metal-free porphyrin (10 μM). ●: control; ●: H_2TMPyP^{4+}; ●: H_2TMAP^{4+}; ●: H_2TCPP^{4-}; ●: H_2TPPS^{4-}.

Effect of zinc or metal-free porphyrin derivatives on the FUM-catalyzed fumarate production based on the L-malate dehydration

The concentration of fumarate produced with FUM after 120 min incubation and the initial rate of fumarate production (v_0), calculated from the fumarate concentration after 5 min incubation in the presence of various porphyrin derivatives were summarized in Table 1.

In the presence of zinc and metal-free porphyrin derivatives, there was no significant difference in FUM-catalyzed production of fumarate from L-malate. Also, it was suggested that cationic zinc and metal-free porphyrin derivatives had no effect on the catalytic activity of FUM for the L-malate dehydration to produce fumarate. For anionic porphyrin derivatives, in contrast, there was a large difference in FUM-catalyzed fumarate production between sulfo and carboxy groups bound to porphyrins or between zinc and metal-free porphyrins. For $ZnTCPP^{4-}$ and H_2TCPP^{4-}, there was no significant difference in FUM-catalyzed production of fumarate from L-malate. Under the addition of $ZnTCPP^{4-}$ and H_2TCPP^{4-}, it was found that the initial rate of fumarate production catalyzed by FUM decreased to about 60–70% compared to the control condition. For $ZnTPPS^{4-}$ and H_2TPPS^{4-}, it was found that the inhibition of FUM-catalyzed fumarate production by addition of $ZnTPPS^{4-}$ had a greater effect than that of H_2TPPS^{4-}. Comparing the initial rate of fumarate production catalyzed by FUM, it decreased about 9 times in the presence of $ZnTPPS^{4-}$ than that of H_2TPPS^{4-}. Moreover, it decreased about 19 times in the presence of $ZnTPPS^{4-}$ than that of control condition in the initial rate of fumarate production catalyzed by FUM. These results suggest that cationic porphyrin derivatives have little effect on FUM-catalyzed fumarate production, regardless of whether zinc-coordinated or metal-free porphyrins. For anionic porphyrin derivatives, in contrast, it was suggested that FUM-catalyzed fumarate production depends on differences in porphyrin skeleton structure, zinc coordination or not.

UV-vis absorption spectrum measurement for the solution of FUM in the addition of water-soluble zinc porphyrin derivatives

Next, $ZnTMAP^{4+}$ and $ZnTPPS^{4-}$ from these porphyrin derivatives were selected and studied their interactions with FUM using spectroscopic techniques. Fig. 7 shows the UV-vis absorption spectra of $ZnTPPS^{4-}$ and $ZnTMAP^{4+}$ (10 μM) in the presence of FUM (0.5 units) in the 500 mM of HEPES buffer solution. UV-vis absorption spectra of $ZnTPPS^{4-}$ and $ZnTMAP^{4+}$ in the absence of FUM as the control samples also are show in Fig. 7(a) and (b). For $ZnTMAP^{4+}$, there was no significant difference in the UV-vis absorption spectra of $ZnTMAP^{4+}$ in the presence and absence of FUM as shown in Fig. 7(b). For $ZnTPPS^{4-}$, in contrast, a slight red shift of the Q bands (557 and 597 nm) of $ZnTPPS^{4-}$ was observed in the presence of FUM. These results suggest a possible electrostatic interaction between FUM and $ZnTPPS^{4-}$. However, because no drastic change was observed in the UV-vis absorption spectral change in the solution of FUM and $ZnTPPS^{4-}$. Therefore, to further clarify the interaction between FUM and $ZnTPPS^{4-}$, analysis by CD spectroscopy was investigated.

Table 1 The concentration of fumarate produced with FUM after 120 min incubation and v_0 in the presence of various porphyrin derivatives

Porphyrin derivatives	[Fumarate] after 120 min (μM)	v_0 (μM min^{-1})
Control	277.9	38.4
$ZnTMPyP^{4+}$	294.3	41.4
$ZnTMAP^{4+}$	284.6	41.7
$ZnTCPP^{4-}$	248.4	25.9
$ZnTPPS^{4-}$	45.50	2.02
H_2TMPyP^{4+}	297.3	36.1
H_2TMAP^{4+}	301.1	37.0
H_2TCPP^{4-}	261.9	21.7
H_2TPPS^{4-}	198.1	18.3

CD spectroscopy measurement for the solution of FUM in the presence of water-soluble zinc porphyrin derivatives

It has been reported that FUM has two different substrate binding sites (sites A and B) with different affinities, (site A has catalytic activity, whereas site B has no catalytic activity) and the

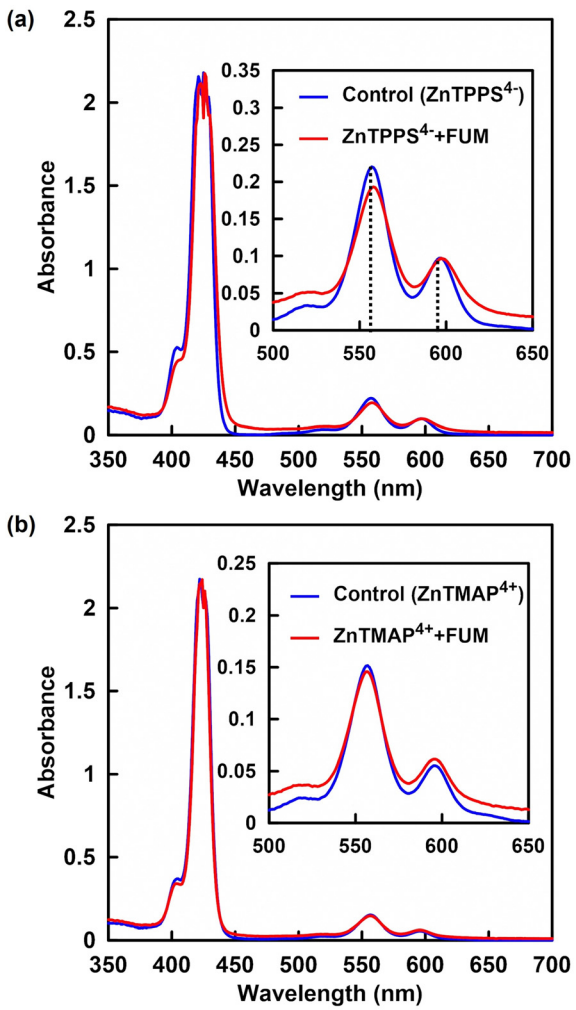

Fig. 7 UV-vis absorption spectra of $ZnTPPS^{4-}$ (a) and $ZnTMAP^{4+}$ (b) in the presence of FUM in the HEPES buffer solution (red line). Blue line: without FUM.

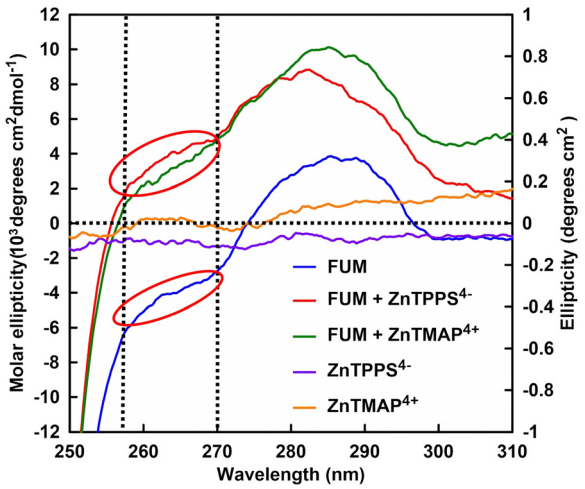

Fig. 8 CD spectra of FUM in the presence of $ZnTMAP^{4+}$ or $ZnTPPS^{4-}$ in the HEPES buffer solution. CD specra of FUM (blue), $ZnTMAP^{4+}$ (orange) and $ZnTPPS^{4-}$ (purple) as the control samples.

interactions between various ligands and substrate-binding sites have been investigated by CD spectroscopy.[18] Fig. 8 shows the CD spectra in near-UV region of FUM (0.75 μM;) in the presence of $ZnTMAP^{4+}$ or $ZnTPPS^{4-}$ using a spectropolarimeter with a 1.0 nm excitation bandwidth at 4 °C. CD spectra of FUM, $ZnTPPS^{4-}$ and $ZnTMAP^{4+}$ as the control samples also are shown in Fig. 8.

In previous reports, the interaction between FUM and ligands was investigated by CD spectral changes between 250 and 310 nm in the near-UV region.[37] It has been reported that the 250 to 270 nm band in the CD spectrum of FUM is enhanced by ligand binding to the substrate binding site due to L-histidine residue in site A.[37]

As shown in Fig. 8, no significant change in CD spectral shape of FUM was observed with the addition of $ZnTMAP^{4+}$. On the other hand, 255 to 270 nm band in the CD spectrum of FUM was changed with the addition of $ZnTPPS^{4-}$ (indicated red circle). These suggest that the binding of $ZnTPPS^{4-}$ to site A with catalytic activity in FUM, inhibits L-malate binding to site A. Tetracarboxylic acid, benzene-1,2,4,5-tetracarboxylate and sulfate have been reported as inhibitors for FUM. Especially, it has been found that one molecule of benzene-1,2,4,5-tetracarboxylic acid can bind to the A and B sites simultaneously and that four molecules per FUM molecule bind with high affinity like a bridge between the two subunits.[37] These results suggest that $ZnTPPS^{4-}$ with four benzenesulfonate moieties also binds to the substrate-binding site of FUM (sites A and B) with high affinity, inhibits dehydration of L-malate, and reduces fumarate production.

Conclusions

In conclusion, the effects of various water-soluble zinc or metal-free porphyrin derivatives additions on fumarate production based on FUM-catalyzed L-malate dehydration was clarified. It was found that the addition of cationic water-soluble porphyrin $ZnTMAP^{4+}$, $ZnTMPyP^{4+}$, H_2TMAP^{4+} or H_2TMPyP^{4+} had little effect on the catalytic activity of FUM for L-malate dehydration to fumarate. On the other hand, it was also found that the addition of anionic water-soluble porphyrin $ZnTCPP^{4-}$, $ZnTPPS^{4-}$, H_2TCPP^{4-} or H_2TPPS^{4-} inhibited the catalytic activity of FUM. Especially, $ZnTPPS^{4-}$ strongly inhibited the catalytic activity of FUM. By adding $ZnTPPS^{4-}$ to the solution containing FUM and L-malate, the concentration of fumarate production after 120 min incubation was reduced to about 16% compared to that in the condition without $ZnTPPS^{4-}$. Also the initial rate of fumarate production with FUM in the presence of $ZnTPPS^{4-}$ was slowed down by 5% compared to that in the condition without $ZnTPPS^{4-}$. Furthermore, spectroscopic results suggested that $ZnTPPS^{4-}$ binds to the substrate-binding site of FUM and inhibits fumarate production. These results contribute to the appropriate selection of the photosensitizing molecule and yield improvement in the visible-light driven fumarate production system as shown in Fig. 3.

Conflicts of interest

There are no conflicts to declare.

Acknowledgements

The authors would like to thank Associate Professor Ritsuko Fujii of Osaka Metropolitan University and Mr Soichiro Seki of Osaka City University for their cooperation in CD spectra measurements. This work was partially supported by Grant-in-Aid for Scientific Research (B) (22H01872), (22H01871), Fund for the Promotion of Joint International Research (Fostering Joint International Research (B))(19KK0144) and Specially Promoted Research (23H05404), and by Institute for Fermentation, Osaka (IFO) (G-2023-3-050).

Notes and references

1 B. D. Ahn, S. H. Kim, Y. H. Kim and J. S. Yang, *J. Appl. Polym. Sci.*, 2001, **82**, 2808.
2 I. Bechthold, K. Bretz, S. Kabasci, R. Kopitzky and A. Springer, *Chem. Eng. Technol.*, 2008, **31**, 647.
3 Y. Jiang, A. J. J. Woortman, G. O. R. Alberda van Ekenstein and K. Loos, *Polym. Chem.*, 2015, **6**, 5451.
4 A. Pellis, A. E. Herrero, L. Gardossi, V. Ferrario and G. M. Guebitz, *Polym. Int.*, 2016, **65**, 861.
5 N. A. Rorrer, J. R. Dorgan, D. R. Vardon, C. R. Martinez, Y. Yang and G. T. Beckham, *ACS Sustainable Chem. Eng.*, 2016, **4**, 6867.
6 L. C. Zheng, Z. D. Wang, C. C. Li, Y. N. Xiao, D. Zhang and G. H. Guan, *Polymer*, 2013, **54**, 631.
7 H. M. Ye, R. D. Wang, J. Liu, J. Xu and B. H. Guo, *Macromolecules*, 2012, **45**, 5667.
8 L. C. Zheng, Z. D. Wang, C. C. Li, D. Zhang and Y. N. Xiao, *Ind. Eng. Chem. Res.*, 2012, **51**, 14107.
9 M. S. Nikolic, D. Poleti and J. Djonlagic, *Eur. Polym. J.*, 2003, **39**, 2183.

10 L. Zheng, Z. Wang, S. Wu, C. Li, D. Zhang and Y. Xiao, *Ind. Eng. Chem. Res.*, 2013, **52**, 6147.
11 P. J. Mann and B. Woolf, *Biochem. J.*, 1930, **24**, 427.
12 S. A. Woods, S. D. Schwartzbach and J. R. Guest, *Biochim. Biophys. Acta*, 1988, **954**, 14.
13 J. S. Keruchenko, I. D. Keruchenko, K. L. Gladilin, V. Zaitsev and N. Y. Chiragadze, *Biochim. Biophys. Acta*, 1992, **1122**, 85.
14 T. Mizobata, T. Fujioka, F. Yamasaki, M. Hidaka, J. Nagai and Y. Kawata, *Arch. Biochem. Biophys.*, 1998, **355**, 49.
15 M. Mescam, K. Vinnakota and D. Beard, *J. Biol. Chem.*, 2011, **286**, 21100.
16 V. P. Veetil, G. Fibriansah, H. Raj, A. M. W. H. Thunnissen and G. J. Poelarends, *Biochemistry*, 2012, **51**, 4237.
17 M. A. Ajalla Aleixo, V. L. Rangel, J. K. Rustiguel, R. A. P. de Pádua and M. C. Nonato, *FEBS J.*, 2019, **286**, 1925.
18 J. A. Milne and R. A. Cook, *Biochemistry*, 1979, **18**, 3605.
19 M. A. Tronconi, M. C. Gerrard Wheeler, V. G. Maurino, M. F. Drincovich and C. S. Andreo, *Biochem. J.*, 2010, **430**, 295.
20 Z. Fu, Z. Zhang, Z. Liu, X. Hu and P. Xu, *Biol. Plant.*, 2011, **55**, 196.
21 Y. Wang, S. P. Long and X. G. Zhu, *Plant Physiol.*, 2014, **164**, 2231.
22 Y. Morimoto, K. Honda, X. Ye, K. Okano and H. Ohtake, *J. Biosci. Bioeng.*, 2014, **117**, 147.
23 Y. Liu, J. Song, T. Tan and L. Liu, *Appl. Biochem. Biotechnol.*, 2015, **175**, 2823.
24 M. Takeuchi and Y. Amao, *React. Chem. Eng.*, 2022, **7**, 1931.
25 M. Takeuchi and Y. Amao, *RSC Sustainability*, 2023, **1**, 90.
26 N. Singh, D. Yadav, S. V. Mulay, J. Y. Kim, N. J. Park and J. O. Baeg, *ACS Appl. Mater. Interfaces*, 2021, **13**, 14122.
27 R. Ruppert, S. Herrmann and E. Steckhan, *Tetrahedron Lett.*, 1987, **28**, 6583.
28 E. Steckhan, S. Herrmann, R. Ruppert, J. Thömmes and C. Wandrey, *Angew. Chem., Int. Ed. Engl.*, 1990, **29**, 388.
29 H. C. Lo, O. Buriez, J. B. Kerr and R. H. Fish, *Angew. Chem., Int. Ed.*, 1999, **38**, 1429.
30 H. C. Lo, C. Leiva, O. Buriez, J. B. Kerr, M. M. Olmstead and R. H. Fish, *Inorg. Chem.*, 2001, **40**, 6705.
31 C. L. Pitman, O. N. L. Finster and A. J. M. Miller, *Chem. Commun.*, 2016, **52**, 9105.
32 T. Katagiri, Y. Kita and Y. Amao, *Catal. Today*, 2023, **410**, 289.
33 Y. Kita and Y. Amao, *Chem. Commun.*, 2022, **58**, 11131.
34 Y. Kita and Y. Amao, *Green Chem.*, 2023, **25**, 2699.
35 M. Takeuchi and Y. Amao, *Sustainable Energy Fuels*, 2023, **7**, 355.
36 J. C. Sacchettini, M. W. Frazier, D. C. Chiara, L. J. Banaszak and G. A. Grant, *Biochem. Biophys. Res. Commun.*, 1988, **153**, 435.
37 S. Beeckmans and E. Van Driessche, *J. Biol. Chem.*, 1998, **273**, 31661.
38 Y. Amao and I. Okura, *J. Mol. Catal. A: Chem.*, 1996, **105**, 125.
39 M. R. Schreier, B. Pfund, D. M. Steffen and O. S. Wenger, *Inorg. Chem.*, 2023, **62**, 7636.
40 A. Harriman and M. C. Richoux, *J. Photochem.*, 1981, **15**, 335.
41 K. Kalyanasundaram and M. Neumann-Spallart, *J. Phys. Chem.*, 1982, **86**, 5163.
42 K. Kalyanasundaram, *J. Chem. Soc., Faraday Trans. 2*, 1983, **79**, 1365.

